Supplemental Figure 1: Generation of the P900L mutant model

(A) Sanger sequencing tracks indicating heterozygous P900L point mutation. The WT CCG codon is changed to a P900L CTG codon, with the mutation highlighted in blue.

(B) Example gel from restriction enzyme genotyping from WT and P900L/+ ear lysate. Digested WT PCR products are at approximately 285bp and 421bp, whereas P900L PCR products are undigested and remain at the full 706bp.

(C) Representative image of WT and P900L mouse at 30 weeks of age.

(D) Quantification of DNMT3A expression from 2-week cortex by RT-qPCR (n=5/genotype, 3 males, 2 females) and western blot (n=8/genotype, 4 males, 4 females). Student's T-Test; * $p<0.05$.

Box plot indicates 25th percentile, median, and 75th percentile. Whiskers indicate minimum and maximum.

Supplemental Figure 2: P900L mutants do not show activity or anxiety-like phenotypes, but do have changes in social and tactile behaviors

(A-B) Time on a continuous (A) or accelerating (B) rotarod indicates no significant differences between WT and P900L animals.

(C) Walking initiation assay, with time to leave a marked square measured.

(D-F) Genotypes had no significant differences in latency to fall of a (D) ledge, (E) platform, or (F) an inverted screen.

(G-H) Genotypes had no significant differences in time taken to (G) turn and climb down a pole, or (H) time to the top of a 60° or 90° screen.

(I) Time freezing during conditioned fear training, during baseline (before tone and shock) and during tone and shock association training.

(J) Distance traveled during the 3-chamber social approach assay.

(K) Body weights of animals during tube test assay indicate no significant differences between genotypes for the P900L animals vs. WT littermates. Body weight and size can have a significant impact on social hierarchies, and testing was done before mutants increased in size.

(L-N) Measures of volume (L), average frequency (M), and duration (N) of ultrasonic vocalization calls in the WT and P900L animals.

(O-P) Time spent investigating objects in NORT (O) and NOR (P) trials for WT and P900L animals.

(Q) Body weight of R878H animals vs. WT littermates during tube test trials.

(R) Active vs. Passive animal status during R878H or WT wins (see methods).

(S-U) Measures of volume (S), average frequency (T), and duration (U) of ultrasonic vocalization calls in the WT and R878H animals.

(V-W) Time spent investigating objects in NORT (V) and NOR (W) trials for WT and R878H animals.

Bar graphs and line plots indicate mean ± SEM; Box-and-whisker plots indicate mean and quartiles. Detailed statistics, and sample sizes in Supplemental Table 1.

Supplemental Figure 3: P900L and R878H mutants exhibit transcriptional overlap with other models disrupting the neuronal epigenome, and mutants also exhibit specific downregulated effects

(A) Log_2 fold changes in the P900L- and R878H- mutants at genes significantly disrupted upon homozygous KO of DNMT3A in postmitotic neurons (Clemens *et al.*, 2019)

(B) P900L- and R878H-specific downregulated gene sets indicated in purple and teal. Specific genes are defined as those that are significantly downregulated in one mutant, and either significantly unchanged (nominal p-value > 0.5) or upregulated in the other (fold change > 0).

(C) Most significant PANTHER gene ontology (biological process) terms enriched in P900L-specific and R878H-specific downregulated gene lists. No terms were significantly enriched in the P900L-specific downregulated gene sets.

(D) Log_2 fold changes in the P900L- and R878H- mutants at genes significantly disrupted in MeCP2 mutants (Clemens *et al.*, 2019)

(E) Log_2 fold changes in the P900L- and R878H- mutants at genes significantly disrupted in upon homozygous KO of NSD1 in neural progenitors (Hamagami *et al.*, 2023)

Notched box and whisker plots indicate median, interquartile, and confidence interval of median with significance from Wilcox Rank Sum test shown. Detailed statistics, and sample sizes in Supplemental Table 1. ** p<0.01; *** p<0.001; # p<0.0001; ## p<2 e^{-10}

Supplemental Figure 1

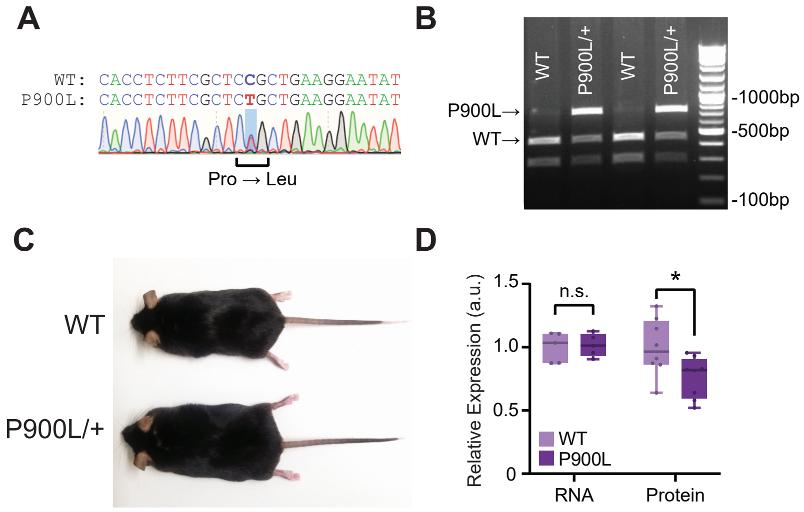

Supplemental Figure 2

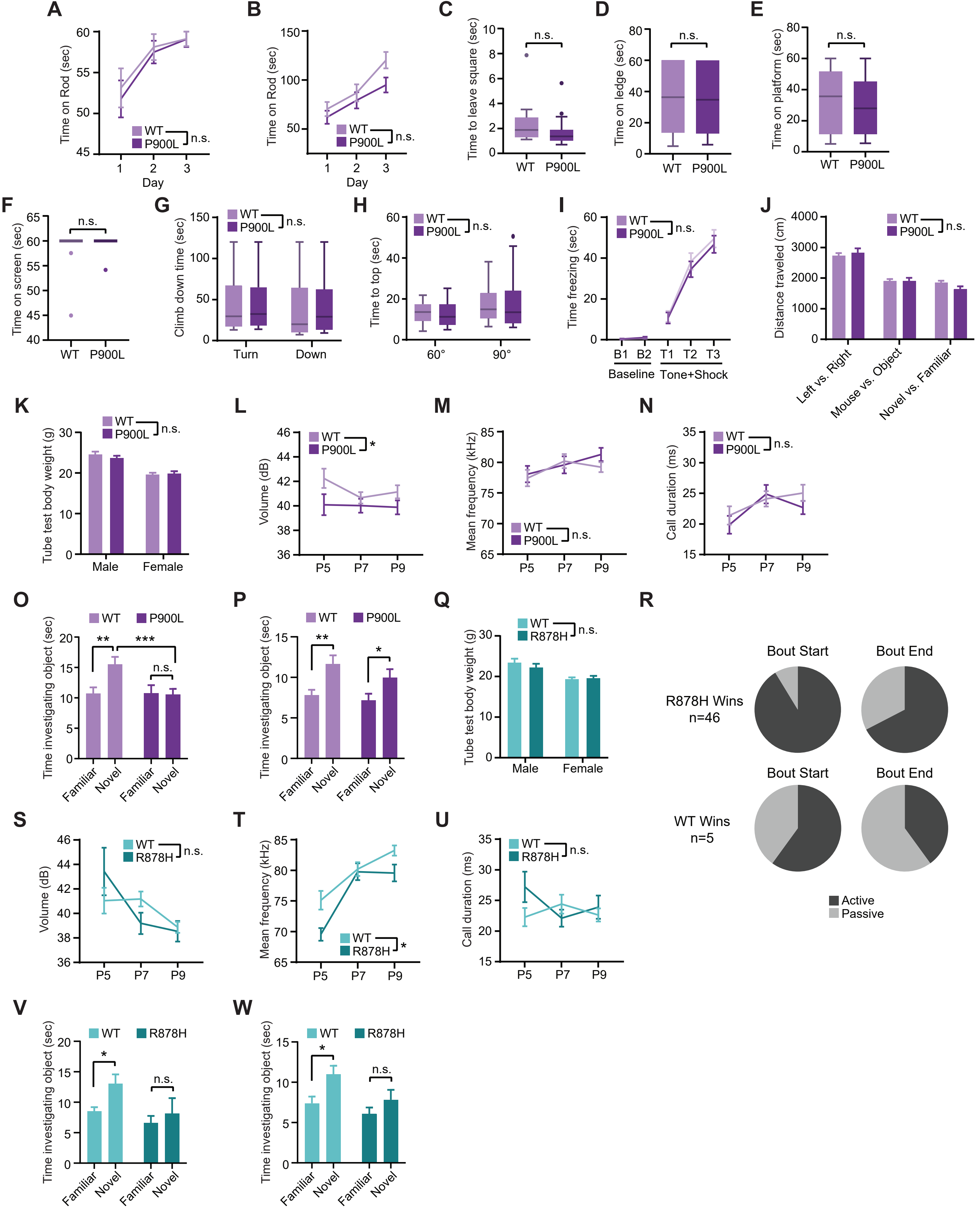

Supplemental Figure 3